Gupta et al., J Proteomics Bioinform 2017, 10:3
DOI: 10.4172/jpb.1000428

Journal of
Proteomics & Bioinformatics

Research Article Open Access

Screening and Identification of Structural Analogs of GW9662 and T0070907 Potent Antagonists of Peroxisome Proliferator-Activated Receptor Gamma: *In-Silico* Drug-Designing Approach

Pramodkumar P Gupta[1*], Shrinkhla Singh[1], Pritam Kumar Panda[1], Danish Ibrahim Jasnaik[1], Santosh S Chhajed[2] and Virupaksha A Bastikar[3]

[1]*School of Biotechnology and Bioinformatics, D Y Patil University, Navi Mumbai, Maharashtra, India*
[2]*Department of Pharmaceutical Chemistry, MET Institute of Pharmacy, Nashik, Maharashtra, India*
[3]*Amity Institute of Biotechnology, Amity University, Mumbai, Maharashtra, India*

Abstract

Peroxisome Proliferator-Activated Receptor Gamma encoded by PPARG gene is also known as type II nuclear receptor in humans plays a significant role in regulating the glucose metabolism, adipocyte differentiation and serves as a lipid sensor. This has been implicated in the pathology of various diseases like obesity, diabetes, atherosclerosis, and cancer. In search of drugs that uses PPAR gamma as a therapeutic target for its inhibition: *In-silico* CADD approaches has been widely used in this aspect to understand the intrinsic molecular aspects and their interaction with the chemicals. *In-silico* based virtual screening helps in identification of optimum molecule among the large dataset to elucidate the effects on a particular target through binding interaction and can be used for further experimentations. In the present study, two PPAR gamma/antagonists GW9662 and T0070907 were selected for this study as they serves as potent therapeutics to minimize the effects of PPAR gamma in chronic diseases. A set of structural analogs of GW9662 and T0070907 were screened from ZINC public database. Ligand based screening is followed by 80% similarity search, Lipinski filter, Pharmacophore based and toxicity based screening. Structure based virtual screening follows the output and final molecular docking using iGemdock and Autodock explained the binding affinity and pharmacological interactions. The results between the GW9662, T0070907 and screened structural analogs show better binding affinity with respect to the former one with similar pharmacological interactions.

Keywords: GW9662; T0070907; PPAR gamma; Virtual Screening; Molecular docking

Introduction

Breast cancer is measured as the most widespread cancer in women, with an estimate of 1.38 million new cases per year across the globe [1]. Usually classified on the basis of clinical features and histopathological findings, but an escalation has been seen that in cellular and molecular characteristics which are of significant importance. Estrogen alpha receptor is considered as the standard biomarker in prediction of breast cancer in response to endocrine treatment and has been found to be expressed in 70-80% of patient suffering from breast cancer. There are significant proportions of ER-positive tumours which are resistant to endocrine therapy, either anew or acquired, and more specific biomarkers as well as new therapeutic targets for endocrine-resistant tumours are needed [2]. The mechanisms of endocrine resistance include loss of ER expression or expression of truncated ER isoforms, post translational alteration or modification of the ER, elimination of cofactors, or overstimulation of tyrosine kinase receptor growth signalling pathways. The peroxisome proliferator-activated receptor γ (PPARγ) ligands show anticancer activity against a wide range of neoplastic cells *in vitro*. Peroxisome proliferator-activated receptor gamma (PPAR-γ or PPARG), also known as the glitazone receptor, orNR1C3 (nuclear receptor subfamily 1, group C, member 3) is a type II nuclear receptor which in humans is encoded by the *PPARG* gene [3]. It is expressed primarily in adipose tissue with less expression in cardiac, skeletal, and smooth muscle cells, islet cells, macrophages, and vascular endothelial cells. Along with adipocyte differentiation, PPAR activity also promotes uptake of circulating fatty acids into fat cells and the shifting of lipid stores from extra-adipose to adipose tissue. The uptake of circulating fatty acids is the basis for the pharmacological application of PPAR gamma in breast cancer patients. It is regulated by ligand binding and post-translational modifications [4]. The previous demonstration shows that endogenous transactivation promotes an aggressive phenotype of malignant breast cells. According to recent findings NR1D1 and the peroxisome proliferator-activated receptor-γ (PPARγ)-Binding Protein (PBP) both act through a common pathway and are responsible for upregulating several genes in the *de novo* fatty acid synthesis network, which is said to be highly active in ERBB2-positive breast cancer cells [4]. Both NR1D1 and PBP are functionally related to PPARγ, which is a well-established positive regulator of adipogenesis and lipid storage. The PPARγ pathway is responsible for reduction of Aldehyde Dehydrogenase (ALDH)-positive population in ERBB2-positive breast cancer cells. The *in vitro* tumorsphere formation assay shows that the two antagonist of PPARγ namely GW9662 and T0070907 are responsible for deduction of tumorsphere formation in ERBB2-positive cells, but not other breast cell [4]. Now talking about the two antagonists GW9662 and T0070907, GW9662 is potent antagonist which shows the inhibition of growing breast tumour cells and also promotes the anticancer effects of the PPARγ agonist rosiglitazone, independent of PPARγ activation [5]. Whereas T0070907 helps in suppression of breast cancer cell proliferation and motility via PPAR

***Corresponding author:** Gupta PP, School of Biotechnology and Bioinformatics, D Y Patil University, Navi Mumbai, Maharashtra, India, Tel: 9920087817; E-mail: pramodkumar785@gmail.com; pramod.gupta@dypatil.edu

Received January 24, 2017; **Accepted** March 28, 2017; **Published** March 31, 2017

Citation: Gupta PP, Singh S, Panda PK, Jasnaik DI, Chhajed SS, et al. (2017) Screening and Identification of Structural Analogs of GW9662 and T0070907 Potent Antagonists of Peroxisome Proliferator-Activated Receptor Gamma: *In-Silico* Drug-Designing Approach. J Proteomics Bioinform 10: 85-93. doi: 10.4172/jpb.1000428

gamma-dependent as well as independent mechanisms [6]. The present work is aim to identify the diverse Structural analogs of GW9662 and T0070907 from public database that can act as prominent Antagonists to PPAR gamma.

Material and Methods

Selection of target

As per the literature review the Crystal Structure of PPAR gamma complexed with Telmisartan is downloaded from protein data bank with pdb_id 3VN2 an x-ray diffraction data at resolution 2.18 Angstrom [7]. It is a selective angiotensin II type 1 receptor blocker. Recently it was reported that telmisartan acts as agonist for PPAR gamma [8].

Active site identification

The active site residues of the Crystal Structure of PPAR gamma complexed with Telmisartan was predicted using Cast-P sever (Computer Atlas of Surface Topology of Proteins) [9], with probe radius 1.4 Armstrong, and validated through Auto dock 4.1 [10] and Discovery studio visualizer 4.0 [11].

Selection of ligands

PPAR gamma Antagonists: In this present study we have considered molecules they are GW9662 and T0070907 [5,6]. GW9662 is an irreversible PPARγ antagonist and inhibits connective tissue growth factor and activation of CD36 by IL-4 (Figure 1) and shows PPAR alpha agonist activity [5]. Whereas T0070907 (Figure 2) is very similar in structure and activity to PPARgamma antagonist GW 96662. It is more potent and has higher selectivity for PPAR gamma over all other subtypes that are about 800 fold more [6]. Based on GW9662 and T0070907 their structural analogs were retrieved from ZINC database [12].

Data mining of ligands

Ligand based screening: Mining of optimum ligand structural analogs from public domain database is a difficult task. ZINC is public database which consist of more than 35 million commercial data sets and non-redundant datasets at noncommercial charges and hence mining of dataset from this database helps in acquiring a less non – redundant datasets [12].

An 80% similarity search was performed using ZINC database against GW9662 and T0070907, resulting in more than 1000 molecules were screened from 35 million compounds. Whereas a second pass filter was carried with property based activity and drug likeness features were exhibited (Table 1): a) Molecular weight; b) Logarithm of the calculated n-octanol/water partition coefficient; c) Number of hydrogen bond acceptors; d) Number of hydrogen bond donors; and e) Number of rotatable single bonds.

Being with two pass filter the screened compounds still showed

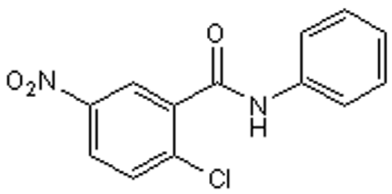

Figure 1: GW 9662.

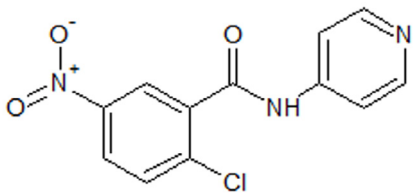

Figure 2: T0070907.

Properties	Minimum	Maximum
MWa	180	500
log P	-0.4	+5.6
HBAc	0	10
HBDd	0	5
NRBe	0	10

Table 1: Summary of physicochemical properties (Often used to predict "Drug-Likeness").

some structural diversity at the basic scaffold level. Hence, Considering a basic scaffold one to one screening was carried out on the basis of basic scaffold of structure and out of 500 molecules 146 molecules were screened, 62 belonging to GW9662 and 84 molecules belonging to T0070907 (Table 2). Filtering the duplication of molecules using ZINC-id 05 molecules identified as common in both the list and total 141 molecules were subjected for the analysis.

Pharmacophore based screening: A 2D structure of 141 structural analogs of GW9662 and T0070907 were sketched using Chemsketch [13] and 3D optimization is carried out using Merck molecular force field (MMFF) in Ligand Scout [14]. A pharmacophore model is created with following features: hydrogen bond donors (HBD), hydrogen bond acceptors (HBA), ring aromatic (RA), and hydrophobic (HY), by considering GW9662 one of the dataset in training and T0070907 as one of the test set condition with 70% and 30% to identify the most closest aligned Pharmacophore model.

Toxicity based screening: The theoretical toxicity based screening was calculated for 92 structural analogs using OSIRIS property explorer (http://www.organic-chemistry.org/prog/peo/) [15], and represented by toxicity risks (mutagenic, irritant, tumorigenic and reproductive effects), states high, medium and low risks profile.

OSIRIS compares input dataset with predefined four subsets of the chemical datasets from RTECS database; they are 7504 mutagenic compounds, 2841 tumorogenic compounds, 2372 irritant compounds and 3570 reproductive effective compounds [15]. The prediction process relies on a precomputed set of 5300 structural fragments from RTECS database datasets that are known to be active in a certain toxicity class and give rise to toxicity alerts in case if they meet in the input structural data [15].

Structure based screening and molecular docking study: Molecular interactions plays an important role in all biological reactions. Drugs are either mimicking or copying the effect of native ligands binding to the receptor by applying the pharmacological and biological reactions. Computational approaches are used to recognize and understand this mode of binding, interacting and multiple

S. No.	ZINC-id	S. No.	ZINC-id	S. No.	ZINC-id	S. No.	ZINC-id
1	ZINC00003381	37	ZINC35279453	73	ZINC78711287	109	ZINC08166092
2	ZINC00039173	38	ZINC37032921	74	ZINC80177501	110	ZINC08424193
3	ZINC00103118	39	ZINC37032925	75	ZINC80177506	111	ZINC13624060
4	ZINC00103124	40	ZINC37247723	76	ZINC81688589	112	ZINC15538832
5	ZINC00225355	41	ZINC37250760	77	ZINC82115191	113	ZINC19230212
6	ZINC00240687	42	ZINC37286046	78	ZINC82262180	114	ZINC19260792
7	ZINC00242270	43	ZINC37673015	79	ZINC82264113	115	ZINC19264532
8	ZINC00266758	44	ZINC37778784	80	ZINC82698016	116	ZINC19392770
9	ZINC00290615	45	ZINC37778789	81	ZINC91495084	117	ZINC19399505
10	ZINC00377492	46	ZINC37995873	82	ZINC92348575	118	ZINC19427956
11	ZINC00434561	47	ZINC40292647	83	ZINC92349427	119	ZINC19477700
12	ZINC00438391	48	ZINC40292649	84	ZINC94665032	120	ZINC20194110
13	ZINC00458448	49	ZINC47916551	85	ZINC00091503	121	ZINC20194113
14	ZINC01056124	50	ZINC49157598	86	ZINC00101971	122	ZINC20194128
15	ZINC01994110	51	ZINC49317454	87	ZINC00103088	123	ZINC20194139
16	ZINC03153944	52	ZINC49376264	88	ZINC00103094	124	ZINC20194142
17	ZINC04045634	53	ZINC50700058	89	ZINC00103103	125	ZINC20194166
18	ZINC05800824	54	ZINC54414540	90	ZINC00103116	126	ZINC20194169
19	ZINC06715798	55	ZINC61680394	91	ZINC00126121	127	ZINC20194214
20	ZINC08780493	56	ZINC62725653	92	ZINC00168318	128	ZINC20194217
21	ZINC09497554	57	ZINC62725669	93	ZINC00231396	129	ZINC20194220
22	ZINC12223463	58	ZINC62725736	94	ZINC00259707	130	ZINC20194223
23	ZINC12620369	59	ZINC62725751	95	ZINC00268121	131	ZINC20194235
24	ZINC16604122	60	ZINC63063491	96	ZINC00293261	132	ZINC20194280
25	ZINC17584697	61	ZINC69771610	97	ZINC00375580	133	ZINC20475562
26	ZINC19470368	62	ZINC70073342	98	ZINC00433206	134	ZINC20478180
27	ZINC19478031	63	ZINC70160175	99	ZINC00438022	135	ZINC36282691
28	ZINC20194172	64	ZINC70230817	100	ZINC00438645	136	ZINC37767839
29	ZINC21959624	65	ZINC70231003	101	ZINC00442284	137	ZINC40311239
30	ZINC21968551	66	ZINC71412398	102	ZINC00456001	138	ZINC40311732
31	ZINC22141304	67	ZINC71414120	103	ZINC00493277	139	ZINC40311738
32	ZINC22148806	68	ZINC73846507	104	ZINC01216529	140	ZINC40311787
33	ZINC23634253	69	ZINC73846563	105	ZINC01227343	141	ZINC50225099
34	ZINC29017357	70	ZINC73846631	106	ZINC02573600		
35	ZINC29020806	71	ZINC73847263	107	ZINC05538460		
36	ZINC35121683	72	ZINC78645916	108	ZINC05672437		

Table 2: Structural analogs of GW9662 and T0070907.

conformations of ligands into the active site to their receptors which is called as Molecular Docking [16,17].

As pharmacological interactions are useful for understanding ligand binding mechanisms to a therapeutic target. These interactions are often inferred from a set of active compounds that were acquired experimentally. Moreover, most docking programs loosely coupled the stages (binding-site and ligand preparations, virtual screening, and post-screening analysis) of structure-based virtual screening (VS). iGEMDOCK is an integrated virtual screening environment from preparations through post-screening analysis with types of bonding and pharmacological interactions [18]. To initially screen on the basis of binding energy and types of bonding we selected the therapeutic protein target 3VN2.pdb [7] and 52 low toxicity risk structural analogs of GW9662 and T0070907. After the generations of the profiles, the compounds were finally subjected to second pass molecular docking, which is carried out using Auto dock 4.1. [10].

Results and Discussion

Active site

The predicted size of active site with an area of 3045.3 and a volume of 4343.7 units Armstrong followed by the input co-ordinates in Auto dock: x=45.444; y=21.713 and z=26.876 respectively and size value of 40 to all the coordinate space (Figure 3), with the following residual information in Table 3.

Ligand based screening

Mining a data set from over a 35 million compounds is a difficult task, but with a ligand structure based similarity search of 80% has

revealed the ease ness of compound selection with an additional filters of physiochemical properties based too. A set of more than 1000 compounds/structural analogs of GW9662 and T0070907 compounds been reduced to set of 500 compounds. With the one to one selection criteria considering the basic scaffold as a prime target the compounds were more refined and 146 total compounds, 62 belonging to GW9662 and 84 molecules belonging to T0070907. Filtering with ZINC-id, 5 duplicates were removed and total 141 compounds were further considered for analysis.

Based on pharmacophore features HBD, HBA, RA and HY alignment in Ligand scout exhibited 92 structural analogs with closest structural feature analogs of GW9662 and T0070907 (Figure 4).

Toxicity prediction: These entire 92 molecules is dividing in two set of toxicity level tested via OSIRIS online tool grouping 40 compounds with high risk to toxicity level for mutagenic, irritant, tumorogenic and reproductive effects, and 52 compounds with low risk to toxicity level (Table 4).

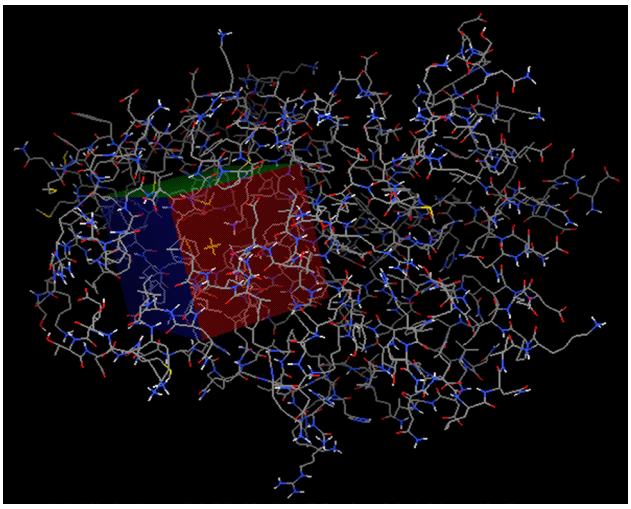

Figure 3: Active site region of PPAR-gamma (Pdb-id: 3VN2).

Amino acid	Amino acid	Amino acid	Amino acid
1	TYR (222)	28	HIS (323)
2	PHE (226)	29	ILE (326)
3	PRO (227)	30	TYR (327)
4	LEU (228)	31	MET (329)
5	THR (229)	32	LEU (340)
6	LYS (230)	33	ILE (341)
7	ILE (249)	34	SER (342)
8	LEU (255)	35	GLU (343)
9	GLY (258)	36	MET (348)
10	GLU (259)	37	ARG (350)
11	ILE (262)	38	LEU (353)
12	ALA (278)	39	LYS (354)
13	ARG (280)	40	LEU(356)
14	ILE (281)	41	PHE (360)
15	PHE (282)	42	GLY (361)
16	GLU (284)	43	PHE (363)
17	CYS (285)	44	MET (364)
18	GLN (286)	45	GLU (365)
19	PHE (287)	46	LYS (367)
20	ARG (288)	47	PHE (368)
21	SER (289)	48	LEU (381)
22	GLU (291)	49	HIS (449)
23	ALA (292)	50	LEU (453)
24	VAL (293)	51	LEU (465)
25	GLU (295)	52	LEU (469)
26	ILE (296)	53	ILE (472)
27	VAL (322)	54	TYR (473).

Table 3: Active site residues.

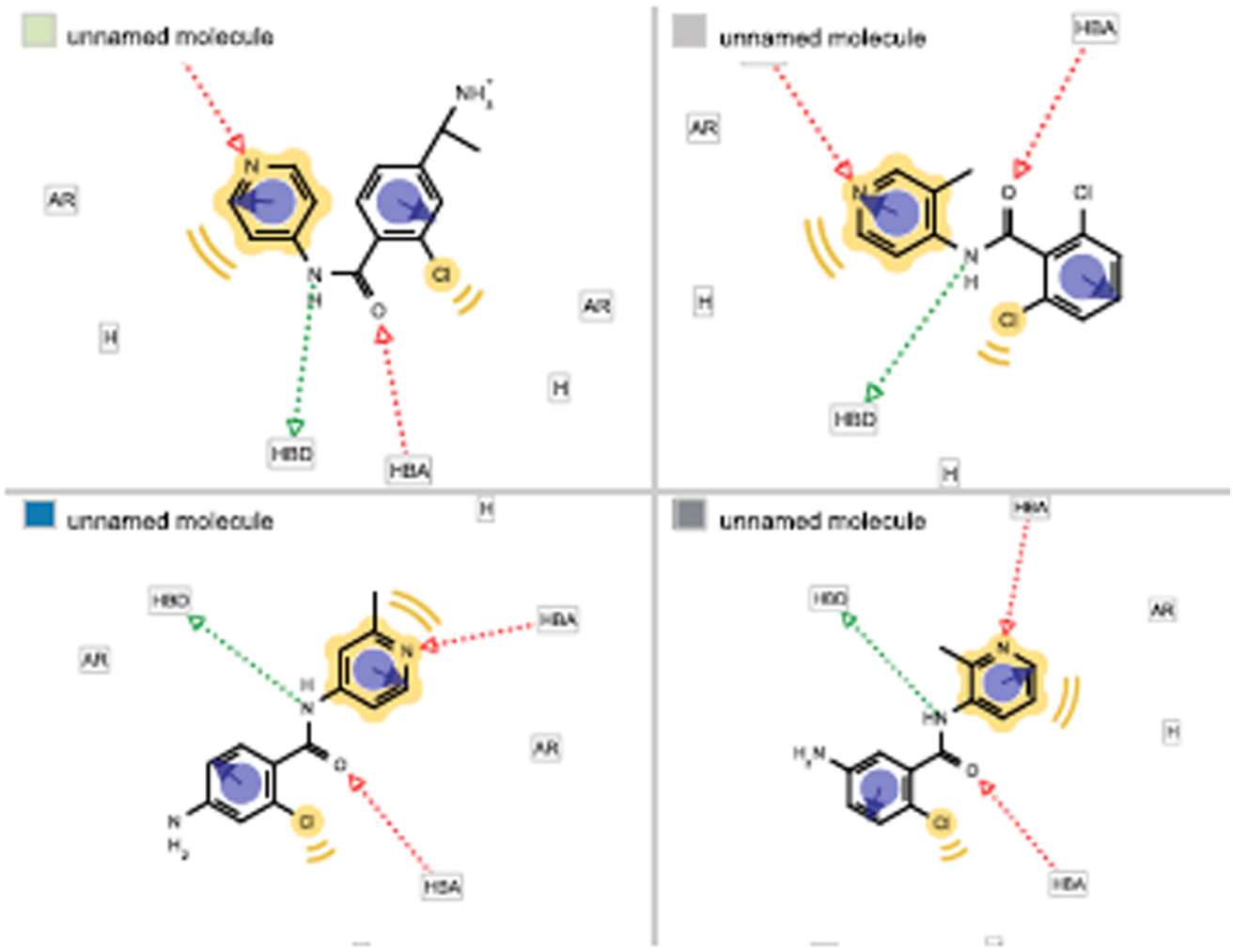

Figure 4: Aligned pharmacophore model.

Structure based screening

Determining the structure based virtual screening, here we submitted 52 low risk compounds for screening, the output from IGemdock resulted in a good prediction of binding energy and exhibited the hydrogen bond, Vanderwaal and electro-static interactions with the receptor and ligand (Table 5).

Molecular docking study

The final docking study was performed on Auto dock 4.1 running on Windows 7. The Auto dock 4.1 uses an evolutionary genetic algorithm approximates a systematic search of positions, orientations and conformations of the ligand in the receptor-binding pocket via a series of hierarchical filters. The shape and properties of the binding site from receptor protein are represented on a grid by a rectangular box confining the translations of the mass center of the ligand. A set of initial ligand conformations or poses were created, of which the most accurately binded ligand pose are selected on the basis of minimum binding energy and desired pharmacological interactions were studied. The binding energy for GW9662 and T0070907 is 9.0 and 8.5 KJ/mol, whereas the ZINC00293261 (Figure 5), ZINC05672437 (Figure 6), ZINC00103124, ZINC29020806, ZINC00438391, ZINC03153944, ZINC35121683 and ZINC37250760 exhibits a more stable energy with binding energy value of -10.7, -10.1, -9.8, -9.6, -9.5, -9.3, -9.1 and -9.0 KJ/mol respectively (Table 6).

Pharmacophore based mapping and ligand features mapping has made an enormous knowledge generation in the field of drug screening and development. Where each atom from ligand and receptor protein interaction is considered on the type of bonding and nature of their interactions such as hydrogen bonding, electrostatic interaction, hydrophobic interactions etc. Comparing the 52 structural analogs of GW9662 and T0070907 with low toxicity risk profile 29 molecules appropriately placed them in the cavity of the receptor protein and

S. No.	Molecule with high toxicity risk	S. No.	Molecule with low toxicity risk	S. No.	Molecule with low toxicity risk
1	ZINC00101971	1	ZINC00091503	41	ZINC62725751
2	ZINC00103094	2	ZINC00103088	42	ZINC69771610
3	ZINC00168318	3	ZINC00103103	43	ZINC70231003
4	ZINC00231396	4	ZINC00103124	44	ZINC71414120
5	ZINC00259707	5	ZINC00126121	45	ZINC73846507
6	ZINC00438022	6	ZINC00268121	46	ZINC73846563
7	ZINC00438645	7	ZINC00293261	47	ZINC73846631
8	ZINC00442284	8	ZINC00375580	48	ZINC73847263
9	ZINC00456001	9	ZINC01216529	49	ZINC78645916
10	ZINC08166092	10	ZINC02573600	50	ZINC78711287
11	ZINC19230212	11	ZINC05538460	51	ZINC82115191
12	ZINC19392770	12	ZINC05672437	52	ZINC94665032
13	ZINC19427956	13	ZINC08424193		
14	ZINC20194113	14	ZINC13624060		
15	ZINC20194128	15	ZINC00039173		
16	ZINC20194142	16	ZINC00103118		
17	ZINC20194166	17	ZINC00225355		
18	ZINC20194169	18	ZINC00266758		
19	ZINC20194217	19	ZINC00377492		
20	ZINC20194220	20	ZINC00438391		
21	ZINC20194223	21	ZINC00458448		
22	ZINC20194235	22	ZINC03153944		
23	ZINC20478180	23	ZINC04045634		
24	ZINC40311239	24	ZINC12223463		
25	ZINC40311732	25	ZINC21959624		
26	ZINC40311787	26	ZINC23634253		
27	ZINC63063491	27	ZINC29017357		
28	ZINC00434561	28	ZINC29020806		
29	ZINC09497554	29	ZINC35121683		
30	ZINC17584697	30	ZINC37032921		
31	ZINC21968551	31	ZINC37032925		
32	ZINC22148806	32	ZINC37247723		
33	ZINC37673015	33	ZINC37250760		
34	ZINC40292647	34	ZINC37286046		
35	ZINC54414540	35	ZINC37778784		
36	ZINC62725736	36	ZINC37778789		
37	ZINC70160175	37	ZINC47916551		
38	ZINC70230817	38	ZINC50700058		
39	ZINC91495084	39	ZINC61680394		
40	ZINC92349427	40	ZINC62725669		

Table 4: Results from OSIRIS.

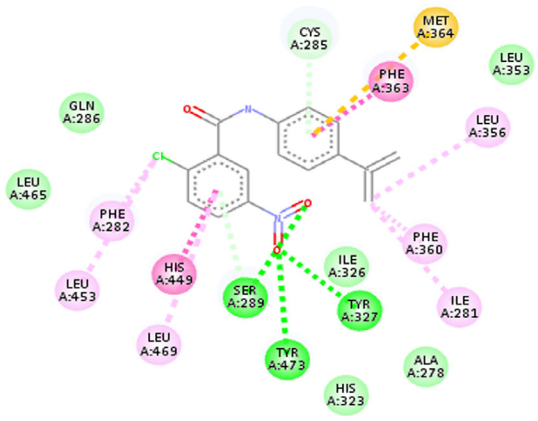

Figure 5: Molecule ZINC00293261 interaction with PPAR-gamma, Pdb-id: 3VN2.

S. No.	Ligands	Total Energy	VDW	HBond	Elec
1	ZINC08424193	-119.544	-108.079	-12.3227	0.858135
2	ZINC00103088	-118.973	-107.122	-12.8735	1.02287
3	ZINC00293261	-118.433	-107.879	-11.6563	1.10243
4	ZINC05672437	-118.087	-102.728	-16.5583	1.19925
5	ZINC13624060	-113.671	-106.244	-7.42713	0
6	ZINC37250760	-110.782	-98.1172	-13.3657	0.701022
7	ZINC00266758	-110.704	-98.0516	-13.353	0.701062
8	ZINC37032921	-109.816	-103.521	-6.2946	0
9	ZINC37032925	-109.706	-103.266	-6.44082	0
10	ZINC94665032	-108.577	-90.9768	-19.0222	1.42239
11	ZINC73846631	-107.334	-99.9581	-7.37555	0
12	ZINC05538460	-107.057	-96.3787	-11.6946	1.01642
13	ZINC73846507	-106.945	-102.002	-4.94304	0
14	ZINC00103118	-106.758	-87.3968	-20.8344	1.47341
15	ZINC00103124	-106.444	-87.9431	-19.948	1.4476
16	ZINC73847263	-106.153	-99.4458	-6.70742	0
17	ZINC78711287	-106.085	-103.713	-2.37159	0
18	ZINC61680394	-105.741	-85.5873	-21.6387	1.48481
19	ZINC37778784	-105.611	-99.184	-6.42655	0
20	ZINC69771610	-105.591	-94.7184	-10.8727	0
21	ZINC50700058	-105.552	-82.2008	-25.1425	1.79108
22	ZINC37778789	-105.528	-99.1107	-6.41745	0
23	ZINC00103103	-105.476	-85.1052	-22.128	1.7567
24	ZINC02573600	-105.338	-105.613	0	0.274777
25	ZINC00225355	-105.3	-91.7738	-14.6161	1.09016
26	ZINC47916551	-103.789	-99.53	-4.25899	0
27	ZINC00268121	-102.408	-92.5018	-10.2201	0.314099
28	ZINC82115191	-102.134	-93.9295	-8.20443	0
29	ZINC00039173	-101.158	-80.8592	-22.052	1.75293
30	ZINC37247723	-101.155	-91.6675	-10.208	0.720593
31	ZINC71414120	-101.029	-101.354	0	0.324669
32	ZINC29017357	-100.804	-96.2192	-4.58458	0
33	ZINC73846563	-100.691	-95.0983	-5.59268	0
34	ZINC01216529	-100.655	-92.831	-8.5	0.675868
35	ZINC37286046	-100.469	-80.1132	-22.1099	1.75373
36	ZINC00438391	-100.326	-88.1606	-13.2737	1.10821
37	ZINC23634253	-100.294	-96.857	-3.4374	0
38	ZINC70231003	-99.1922	-78.0809	-22.4145	1.30312
39	ZINC00458448	-99.1543	-94.9479	-4.20635	0
40	ZINC00375580	-98.7094	-80.191	-19.7748	1.25644
41	ZINC78645916	-98.6416	-97.6431	-0.99846	0
42	ZINC35121683	-98.5428	-95.5498	-2.993	0
43	ZINC29020806	-98.4981	-95.4803	-3.01782	0
44	ZINC00091503	-95.4933	-94.1309	-1.36242	0
45	ZINC62725669	-94.5289	-89.2391	-5.28982	0
46	ZINC00126121	-93.8833	-93.8833	0	0
47	ZINC03153944	-93.6787	12.1913	-2.14548	-0.67793
48	ZINC00377492	-93.4082	-93.4082	0	0
49	ZINC62725751	-93.3056	-87.9294	-5.37627	0
50	ZINC04045634	-91.4898	-88.0334	-3.45643	0
51	ZINC12223463	-83.0465	-79.5647	-3.4818	0
52	ZINC21959624	-82.8496	-82.8496	0	0

Table 5: Result from IGem dock.

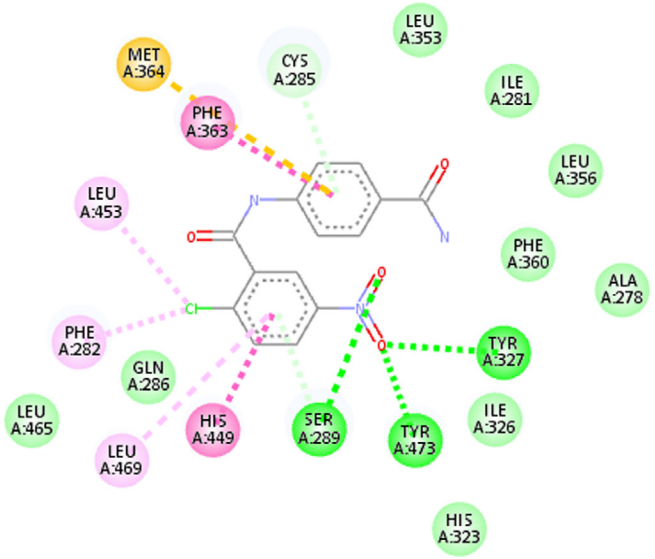

Figure 6: Molecule ZINC05672437 interaction with PPAR-gamma, Pdb-id: 3VN2.

S. No.	Compound	Hydrogen bonding	Pi-interaction	Energy
1	GW9662	TYR 327	CYS 285, PHE 363, MET 364, HIS 449, LEU 453	-9.0
2	T00070907	SER 289, TYR 327, TYR 473	PHE 282, CYS 285, PHE 363, MET 364, HIS 449	-8.5
3	ZINC00293261	CYS 285, SER 289, TYR 327, TYR 473	ILE 281, PHE 282, LEU 356, PHE 360, PHE 363, MET 364, LEU 453, HIS 449, LEU 469	-10.7
4	ZINC05672437	CYS 285, SER 289, TYR 327, TYR 473	PHE 282, PHE 363, MET 364, HIS 449, LEU 453, LEU 469	-10.1
5	ZINC00103124	CYS 285, SER 289, TYR 327, TYR 473	ILE 281, PHE 282, LEU 356, PHE 363, MET 364, HIS 449, LEU 453	-9.8
6	ZINC29020806	CYS 285, TYR 473	PHE 282, CYS 285, PHE 363, MET 364, LEU 453, TYR 473	-9.6
7	ZINC00438391	CYS 285, SER 289, MET 364, TYR 473	PHE 282, CYS 285, PHE 363, MET 364	-9.5
8	ZINC03153944	SER 289, TYR 327, MET 364, TYR 473	CYS 285, PHE 363, MET 364, HIS 449, LEU 469	-9.3
9	ZINC35121683	CYS 285, TYR 327, TYR 473	PHE 282, CYS 285, PHE 363, MET 364, HIS 449, LEU 453, LEU 469	-9.1
10	ZINC37250760	SER 289, TYR 327, TYR 473	ILE 281, PHE 282, CYS 285, PHE 363, MET 364, HIS 449	-9.0
11	ZINC37032925	TYR 327, TYR 473	PHE 282, CYS 285, PHE 363, MET 364, LEU 469, TYR 473	-8.9
12	ZINC23634253	CYS 285	PHE 282, CYS 285, PHE 363, MET 364, HIS 449, LEU 453	-8.7
13	ZINC29017357	CYS 285, TYR 327, PHE 360	CYS 285, LEU 353, PHE 363, MET 364, HIS 449	-8.6
14	ZINC00458448	CYS 285, SER 289, TYR 327, HIS 449, TYR 473	PHE 282, CYS 285, ILE 326, PHE 363, MET 364	-8.6
15	ZINC02573600	ARG 288	CYS 285, ARG 288, ALA 292, ILE 326, MET 329, LEU 330, LEU 333	-8.5
16	ZINC00103088	ARG 288, SER 289, PHE 363	CYS 285, ARG 288, ILE 326, TYR 327, LEU 330	-8.4
17	ZINC12223463	CYS 285	PHE 282, CYS 285, PHE 363, MET 364, HIS 449, LEU 453	-8.3
18	ZINC21959624	CYS 285	PHE 282, CYS 285, PHE 363, MET 364, HIS 449, LEU 453	-8.3
19	ZINC05538460	LEU 228, ARG 288	ALA 292, GLU 295, ILE 326, MET 329, LEU 330, LEU 333	-8.1
20	ZINC37286046	CYS 285, SER 289, TYR 327, TYR 473, HIS 449	ILE 326, PHE 363, MET 364	-7.9
21	ZINC37247723	CYS 285, ARG 288, SER 289	CYS 285, ARG 288, ALA 292, ILE 326, MET 329, LEU 330, VAL 339, MET 364	-7.6
22	ZINC00091503	CYS 285, SER 289, TYR 473	CYS 285, VAL 322, HIS 323, ILE 326, PHE 363, MET 364, HIS 449, LEU 469	-7.6
23	ZINC00126121	ARG 288	ARG 288, ALA 292, GLU 295, ILE 326, MET 329, LEU 330, LEU 333	-7.5
24	ZINC01216529	SER 288	CYS 285, ARG 288, LEU 330, ILE 341	-7.5
25	ZINC00039173	ARG 288, SER 289	CYS 285, ARG 288, TYR 327, LEU 330	-7.5
26	ZINC00375580	ARG 288	CYS 285, ARG 288, ALA 292, ILE 326, LEU 330, ILE 341	-7.4
27	ZINC04045634	CYS 285, SER 289, TYR 473	PHE 282, CYS 285, ILE 326, PHE 363, MET 364, HIS 449, LEU 469	-7.3
28	ZINC00103103	SER 289	CYS 285, ARG 288, LEU 330	-7.1
29	ZINC00434561	ARG 288	LEU 228, ARG 288, ALA 292, GLU 295, ILE 326, MET 329, LEU 330, LEU 333	-7.1
30	ZINC00377492	SER 289	ARG 288, ALA 292, ILE 326, MET 329, LEU 330	-7.0
31	ZINC00225355	SER 342	ILE 281, GLY 284, CYS 285, ARG 288, ILE 341	-6.7

Table 6: Binding energy and interactions between GW9662, T0070907, structural analogs and PPAR-gamma.

forms a hydrogen bonding and pi-interaction and forms similar pharmacophoric interactions as compared to GW9662 and T0070907 with PPAR-gamma receptor protein.

Conclusion

The work presented here was to identify the optimum structural analogs from public database with respect to structural, binding affinity and pharmacological interaction. A number of *in-silico* techniques have been implemented to screen the diverse molecule from the set of molecules. The screening was not dependent on the structural similarity but also on the physio chemical parameters. The pharmacophore model based screening was one where Hydrogen Bond Donors (HBD), Hydrogen Bond Acceptors (HBA), Ring Aromatic (RA), and Hydrophobic (HY) has generated a immense knowledge to screened the most optimum on the basis of these activity. Whereas the criteria for toxicity prediction; Mutagenicity, Tumorigenicity, Irritating effects and Reproductive Effect helped in reducing those dataset which has close structural and physiochemical similarity to the parent one. Finally the structure based screening has generated the most promising results where few structural analogs showed better binding affinity and very close pharmacological interaction patterns with respect to GW9662 and T0070907. Further these molecules could be studied in *in vitro* conditions further to evaluate its detail function over PPAR gamma.

Competing Interests

The author(s) of manuscript "Screening and Identification of Structural Analogs of GW9662 and T0070907 Potent Antagonists of Peroxisome Proliferator-Activated Receptor Gamma: *In silico* Drug-Designing Approach" declare that they have no competing interests.

References

1. Chottanapund S, Van Duursen MB, Navasumrit P, Hunsonti P, Timtavorn S, et al. (2013) Effect of androgens on different breast cancer cells co-cultured with or without breast adipose fibroblasts. J Steroid Biochem Mol Biol 38: 54-62.
2. Karlsson E, Pérez-Tenorio G, Amin R, Bostner J, Skoog L, et al. (2013) The mTOR effectors 4EBP1 and S6K2 are frequently coexpressed, and associated with a poor prognosis and endocrine resistance in breast cancer: a retrospective study including patients from the randomised Stockholm tamoxifen trials. Breast Cancer Res 15: R96.
3. Lee G, Elwood F, McNally J, Weiszmann J, Lindstrom M, et al. (2002) T0070907, a selective ligand for peroxisome proliferator-activated receptor gamma, functions as an antagonist of biochemical and cellular activities. J Biol Chem 277: 19649-19657.
4. Wang X, Sun Y, Wong J, Conklin DS (2013) PPARγ maintains ERBB2-positive breast cancer stem cells. Oncogene 32: 5512-5521.
5. Seargent JM, Yates EA, Gill JH (2004) GW9662, a potent antagonist of PPARγ, inhibits growth of breast tumour cells and promotes the anticancer effects of the PPARγ agonist rosiglitazone, independently of PPARγ activation. Br J Pharmacol 143: 933-937.
6. Zaytseva YY, Wallis NK, Southard RC, Kilgore MW (2011) The PPARgamma antagonist T0070907 suppresses breast cancer cell proliferation and motility via both PPARgamma-dependent and independent mechanisms. Anticancer Res 31: 813-823.
7. Amano Y, Yamaguchi T, Ohno K, Niimi T, Orita M, et al. (2012) Structural basis for telmisartan-mediated partial activation of PPAR gamma. Hypertens Res 35: 715-719.
8. Goebel M, Clemenz M, Staels B, Unger T, Kintscher U, Gust R et al. (2009) Characterization of new PPAR gamma agonists: analysis of telmisartan's structural components. Chem Med Chem. 4: 445-456.
9. Jie L, Herbert E, Clare W (1998) Anatomy of Protein Pockets and Cavities: Measurement of Binding Site Geometry and Implications for Ligand Design. Protein Sci 7: 1884-1897.
10. Morris GM, Huey R, Lindstrom W, Sanner MF, Belew RK, et al. (2009) Autodock4 and AutoDockTools4: automated docking with selective receptor flexibility. J Computational Chem 16: 2785-2791.
11. Accelrys Software Inc. (2013) Discovery Studio Modeling Environment, Release 4.0, San Diego: Accelrys Software Inc.
12. Irwin JJ, Shoichet BK (2005) ZINC–a free database of commercially available compounds for virtual screening. J Chem Inf Model. 45: 177-182.
13. Chemsketch, version 12.0 (2014) Advanced Chemistry Development, Inc., Toronto, On, Canada.
14. Wolber G, Langer T (2005) LigandScout: 3-D pharmacophores derived from protein-bound ligands and their use as virtual screening filters. J Chem Inf Model 45: 160-169.
15. http://www.organic-chemistry.org/prog/peo/%20Accessed
16. Jain A, Gupta PP (2015) *In silico* Comparative Molecular Docking Study and Analysis of Glycyrrhizin from *Abrus precatorius* (L.) against Antidiabetic Activity. Eur J Med Plants 6: 212-222.
17. Panda P, Ibrahim D, Gupta PP (2014) Computational modeling and analysis of theoretical structure of corneodesmosin receptor protein with existing phytochemicals in psoriasis. Indian J Fundamental Appl Life Sci 4: 346-355.
18. Hsu KC, Chen YF, Lin SR, Yang JM (2011) iGEMDOCK: a graphical environment of enhancing GEMDOCK using pharmacological interactions and post-screening analysis. BMC Bioinformatics 12: S33.